

DYNAMIC SIMULATION AND CONTROL SYSTEM MODELLING OF SOLID OXIDE FUEL CELL HYBRIDS

F. Kroll, A. Nielsen, S. Staudacher
 Institute of Aircraft Propulsion Systems (ILA)
 University of Stuttgart
 Pfaffenwaldring 6
 70569 Stuttgart, Germany

OVERVIEW

With the development trend towards “more electric aircrafts” the research for new APU (auxiliary power unit) concepts on the basis of fuel cells receives increasing attention. In this context a hybrid APU consisting of a gas-turbine part coupled to a solid oxide fuel cell (SOFC) promises a significant increase in efficiency. Handling characteristics, transient performance and control concepts of such hybrid power plants provide major challenges which are completed by questions concerning reliability, availability and the minimisation of weight and cost.

The presented paper documents an approach for the real time modelling of a hybrid system as a basis for control system design and optimisation. During the setup of the non-linear model of both, the gas turbine components and the SOFC, the focus was put on a sufficiently accurate reflection of the dynamic effects. On the other hand the model structure was kept lean enough to allow a real time simulation. Furthermore, a modular model set up was maintained to allow easy implementation of possibly necessary additional components and also to adjust the simulation of various operation conditions.

To realise the coupling of gas turbine and SOFC fuel cell a control strategy is presented. Hereby, the control model architecture takes into account the requirements of the gas turbine components but also necessitates safe operation of the SOFC. Since the operation characteristics of both systems are different some important and challenging boundary conditions can be specified. To ensure failure-free and safe operation during the entire operation range these conditions are strictly to be considered within the control structure.

NOMENCLATURE

APU	Auxiliary Power Unit
MGT	Micro Gas Turbine
ODE	Ordinary Differential Equation
SOFC	Solid Oxide Fuel Cell
TOT	Turbine Outlet Temperature

Variables

A	area [m ²]
c	concentration [mol/m ³]
c _p	spec. heat capacity (p=const.) [J/(kg*K)]
c _v	spec. heat capacity (V=const.) [J/(kg*K)]
FU	fuel utilisation [-]
G	plant (model) [-]

h	specific enthalpy [J/kg]
i	current density [A/m ²]
K	controller [-]
I	inertia [kg*m ²]
m	mass [kg]
\dot{m}	mass flow [kg/s]
N	shaft speed [1/s]
P	power [W]
p	pressure [Pa]
\dot{q}	volume flow [m ³ /s]
\dot{r}	reaction rate [mol/s]
R	specific gas constant [J/(kg*K)]
STCR	steam to carbon ratio [-]
t	time [s]
T	temperature [K]
\dot{T}	Time gradient [K/min]
u	actuating variable [-]
U	voltage [V]
v	(internal) commanded variable [-]
V	volume [m ³]
w	commanded variable [-]
y	controlled / measured variable [-]

Greek symbols

α	coefficient of heat transfer [W/m ² *K]
ζ	voltage losses [V]
η	efficiency [-]
λ	stoichiometric air excess ratio [-]
ν	stoichiometric reaction-coefficient [-]
Π	pressure ratio [-]
τ	time constant [1/s]

Subscript

act	activating
cas	casing body
comb	combustor
comp	compressor
el	electric
ex	external
gen	generator
in	inlet
mec	mechanical
mix	mixing
ohm	ohmic
ref	reforming
rev	reversible
t	total
WGS	water-gas-shift

3. MODELLING OF MGT AND SOFC

The models were developed within the MATLAB/Simulink environment to exploit the MATLAB mathematical functions and to create a visual, user-friendly, modular code, allowing any supplements during study work on the hybrid system. Every sub-component of the model is assumed to be adiabatic. The fluid is modelled using temperature dependant properties e.g. c_p . The fuel that is fed to the combustor and the SOFC is regarded as pure methane. The mass flow through the components is determined through the maps of the turbo machines. Changes in the mass flow as a result of volume packing are represented through volumes which are modelled separately [4]. The pressure losses in the component are taken from a map dependent on the mass flow.

3.1. Micro-Gas-Turbine

For gas turbine modelling the micro gas turbine is split into compressor, recuperator, combustor, turbine, shaft and generator. Steady-state performance of the gas turbine depends on the characteristic maps of compressor and turbine and the conversation of energy and mass. The gas turbine components can be described using their state parameters pressure and temperature at component entry and exit. The model techniques for steady state models of these components are well-known and hence not discussed in further detail. The dynamic performance of a gas-turbine is basically determined by the moment of inertia of the rotating components, the heat transfer between fluid and metal and the compressibility effects in the component volumes.

Differential equation (1) describes the change of the shaft speed. It becomes obvious that the moment of inertia of all rotating components dominates the gas turbine transient performance:

$$(1) \quad \frac{dN}{dt} = \frac{\eta_{mec} (P_{turb} - P_{comp}) - P_{gen}}{N(2\pi)^2 I}$$

The defining equations regarding the heat transfer between fluid and engine structure [4] are given with equations (2) and (3):

$$(2) \quad \frac{dT_{cas}}{dt} = \frac{1}{\tau_{cas}} (T_{fluid} - T_{cas})$$

$$(3) \quad \dot{Q}_{cas} = (\alpha A)_{cas} (T_{cas} - T_{fluid})$$

The temperature of the casing T_{cas} is calculated for each component of the system and their change is determined by the time-constant τ_{cas} in equation (2). The transferred amount of heat is given with the heat transfer coefficient, the corresponding area and the temperature difference (see equation 3). The heat transfer has a direct impact on the differential equation for the temperature in each component, which is presented in equation (4) as a deduction of the time dependant first thermodynamic law.

$$(4) \quad \frac{dT_t}{dt} = \frac{1}{c_v m} [\dot{m}_in h_{in} - \dot{m}h + P_{ex} + \dot{Q}_{cas} - c_v (\dot{m}_in - \dot{m})]$$

The power P_{ex} in equation (4) is the sum of all other

powers in the respective component, e.g. the needed power for the compression P_{comp} in the compressor module, the applied energy by the fuel in the combustor or the transferred heat in the recuperator. The specific enthalpy is read out from a pre-calculated map as a polynomial function of the temperature.

Based on the perfect gas equation the differential equation for the pressure can be given in equation (5).

$$(5) \quad \frac{dp_t}{dt} = \frac{R}{V} \left[m \frac{dT_t}{dt} - (\dot{m}_in - \dot{m}) T_t \right]$$

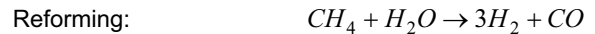
3.2. SOFC

Several papers have been published that focus on detailed models of the SOFC [3, 8]. One objective of this work is to provide a model that satisfies the mass and energy conservation and can display the fundamental dynamic behaviour. Nevertheless the model complexity has to be similar to the models of other parts of the hybrid system and it should be possible to run the thermodynamic model with the control system in real-time.

Hence several assumptions and simplifications for the SOFC have been made. The recirculation rate is constant during transient manoeuvres. Interactions between the cells in the SOFC stack are neglected, that means only one representative cell is calculated. The cell voltage is constant within the whole stack. The pre-reformer (see FIG 1) is not regarded as an independent module. It is assumed, that the whole reforming reaction occurs on the anode side of the SOFC. Furthermore, it is assumed, that CO is not involved in the electrochemical reaction.

The differential equations for the temperatures and pressures at anode and cathode side are analogue to the ones in the modules of the gas turbine with heat transfer to the casing taken into account.

The basic reactions on the anode side of the SOFC can be splitted into the reforming reaction, the electrochemical reaction and the water-gas-shift reaction.



The reaction rate of the reforming reaction is calculated by the common kinetic approach [1] whereas the water-gas-shift reaction is assumed to be always at equilibrium. Therefore the reaction rate can be determined from the change in Gibbs energy [10]. The reaction rate for the electrochemical reaction can be calculated with equation (6).

$$(6) \quad \dot{i}_{el} = \frac{j^* A_{el}}{2 * F}$$

The above listed reactions, the inflow and the outflow change the composition of the gas mixture in the SOFC.

The resulting differential equation for each substance concentration c_i is formulated in equation (7).

$$(7) \quad \frac{dc_i}{dt} = \frac{1}{V} (\dot{q}_{in} c_{i,in} - \dot{q} c_i + v_{i,ref} \dot{r}_{ref} + v_{i,el} \dot{r}_{el} + v_{i,WGS} \dot{r}_{WGS})$$

The correlation between the cell-voltage and the current density j in equation (6) is given by the voltage current characteristics. The cell voltage is also dependent on the temperature and the composition of the involved gases. Equation (8) shows the method of calculating the cell-voltage.

$$(8) \quad U = U_{rev} - \zeta_{ohm} - \zeta_{act} - \zeta_{diff}$$

The actual cell voltage is the difference from the reversible potential U_{rev} and three loss terms, given as ohmic losses ζ_{ohm} [13], activation losses ζ_{act} [13] and diffusion losses ζ_{diff} [12]. To save computation time, the quite complex equations of the different losses are interpolated out from a pre-calculated multidimensional map.

The anode and cathode section of the SOFC consists in only one calculating segment, i.e. there is just one ODE for temperature, pressure and each concentration. The ejector is considered as an ideal mixing section of the recirculated anode exhaust and the fuel flow to the SOFC. At ejector and anode outlet, the gas mixture is assumed to be at the water-gas-shift equilibrium.

4. LIMITATIONS AND BOUNDARY CONDITIONS

The definition of the operational boundaries of the modelled components formed an important basis for the control system design. The safe and reliable operation of the fuel cell resulted in important operational restrictions. High attention was paid to the risk of thermally induced stresses which could result in the destruction of the fuel cell. Furthermore the avoidance of a backflow of gas from the burner to the anode cycle, which would result in the oxidation of the anode was taken into account also.

The limiting values are based on literature [13]. Hence they cannot be regarded as exact values. Adjusting these limits in a small range will result only in the necessity to adjust the time constants of the control loops. Bigger changes might lead to a change in the control concept. The most important boundary conditions for the SOFC are summarized in TAB.1.

Minimum voltage	$U_{min} = 0.6$
Range for the current density	$2000 < i < 4450$
Fuel utilisation limited	$0.7 < FU < 0.9$
Minimum steam-to-carbon-ratio	STCR > 2
Limitations to the stoichiometric air ratio	$\lambda > 2$
No pressure deviation between anode and cathode	$4000 < \Delta p < 10000$

Time-gradient	$\dot{T} < 5$
Local maximum temperature	$T_{max} = 1400$
Temperature at cathode inlet	$T_{min} = 870$

TAB 1. Limitations and boundary conditions for SOFC operation

The operational envelope of the gas turbine has been limited by a maximum shaft speed and maximum limits for the gas temperatures.

5. CONTROL LOOPS

There are several possibilities to correlate the actuating variables and the process variables that need to be controlled in a MGT/SOFC hybrid system depending on the plurality of various hybrid cycle applications. [5, 6, 14]

The used control loops are based on two different control structures. The first one is the standard control cycle in FIG 2.

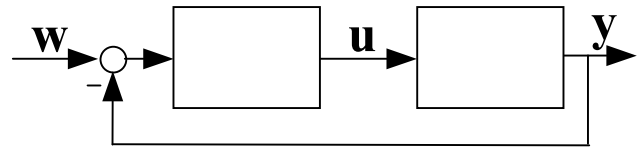


FIG 2. Standard control loop

This standard structure is applied to the following control loops for the system:

- To control the turbine outlet temperature (TOT) to its set-point via adjusting the fuel flow to the MGT combustor
- To keep the fuel utilisation of the SOFC constant by varying the fuel flow to the SOFC
- To ensure no pressure deviations between anode and cathode side of the SOFC by actuating the pressure in fuel supply system with the fuel-compressor
- To reach the demanded SOFC power output by adjusting the SOFC current.

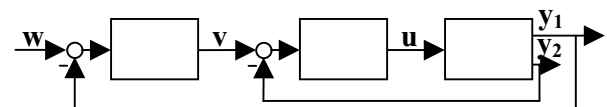


FIG 3. Cascade control loop

A second control structure is applied as a cascade control loop as illustrated in FIG 3. This cascade controller

is used to control two additional system parameters:

- To keep the MGT power output on its set-point. The output of the first controller K_1 is an internal set-point for the shaft-speed which is achieved by varying the generator torque (u). The advantage is the possibility to limit this internal set-point to the maximum shaft speed and to disable the first controller if there is no external MGT power set-point, but an external speed set-point (for example during start-up or shutdown).
- To regulate the SOFC stack temperature. The output of the first controller is a set-point for the air flow through the cathode, which can be monitored and limited in the same way than the shaft speed. This value is compared with the measured air flow. The resulting control error is the origin for calculating the needed bypass ratio around the SOFC by adjusting the control valve. During shutdown procedure, the bypass around the recuperator is used instead.

Most of the restrictions presented in section 4 focus on the SOFC stack temperature, so this variable definitely has to be controlled. Without having the SOFC bypass, the control loop cannot be realised in the illustrated way. Using the generator power (torque) would be the only way to have an influence on the airflow through the cathode, and hence an influence on the stack temperature.

It should be mentioned, that in a first approach the regulation of the SOFC stack temperature is replaced with the regulation of the anode, respectively cathode outlet temperature of the stack. This is a legitimated procedure, because the basic structure of this control loop does not change.

6. SIMULATION RESULTS

To show the functionality of the proposed control strategy, several simulation results of different manoeuvres are presented.

When demand of electric power is changed, the hybrid system must be operated at part-load conditions. Therefore load changes have been simulated to show the behaviour of the system. Three manoeuvres are discussed within this investigation consisting of a small load change, a load-change over a bigger power range and a shutdown manoeuvre. All simulations start at the design point of the hybrid system i.e. the point with maximal power output of the whole system. The changes in load are not directly forced to the system from the demanded net power. They are given changes of the total system power output.

6.1. Small load change

A change in the load set-point of about 10% has been simulated as a representative small load change. Beginning at design point power the power output demand is lowered while keeping the SOFC temperature constant. As illustrated in FIG 4 the sum of the electrical output of the gas turbine and the SOFC follows the net power set-point change without significant deviations. It also can be shown, that the power output of the SOFC does not change during the small change. Such load changes will

be covered by adjusting the power output of the MGT only without changing the load conditions in the SOFC.

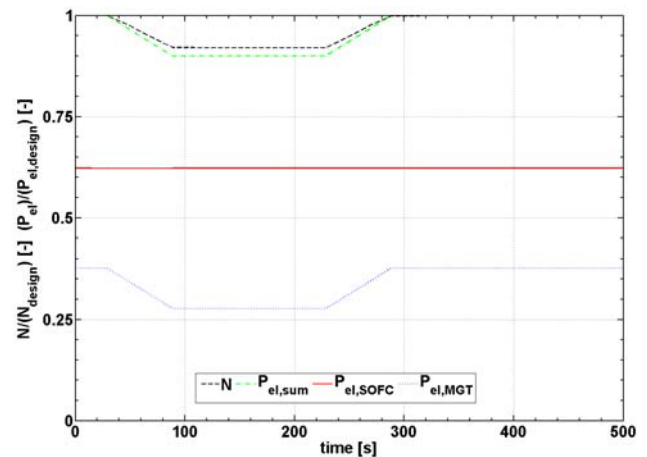


FIG 4. Electrical power output of the hybrid-system and its components for a small load-change

The temperatures around the SOFC stack are shown in FIG 5. The two controlled temperatures (the cathode outlet temperature and the TOT) do not change during the manoeuvre. This, however, is only possible by adjusting the SOFC-bypass. The changes in the resulting mixing temperature T_{mix} result from the control activity of this actuator.

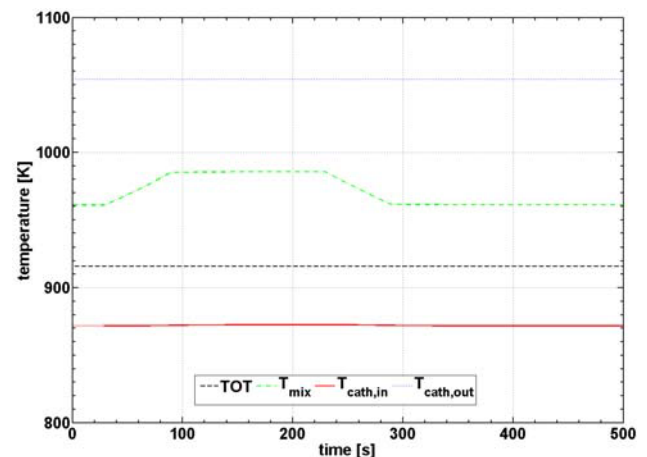


FIG 5. Air-Temperatures around the SOFC-stack and TOT for a small load-change

The change in the internal set-point of the bypass flow is displayed in FIG 6. It should be noted, that although a constant power output and constant stack temperature of the SOFC during the whole simulation, the mass flow to the cathode changes due to the pressure dependence of the cell voltage and voltage losses (decrease in speed).

The influence of the most important control parameters and the operational concept can be discussed based on these figures: To keep preferably many of the SOFC boundary conditions constant (here the temperature and the power), the load change is done via the gas turbine. If the power output of the gas turbine needs to get smaller, the air mass flow through the compressor will decrease. Without adjusting the mass flow through the SOFC bypass, the temperature of the stack will raise up, since

less cooling air will be available. The sum of these effects would influence the SOFC power output and it would not be possible to keep this power constant; hence the internal set-point for the gas turbine power output has to take these effects into account.

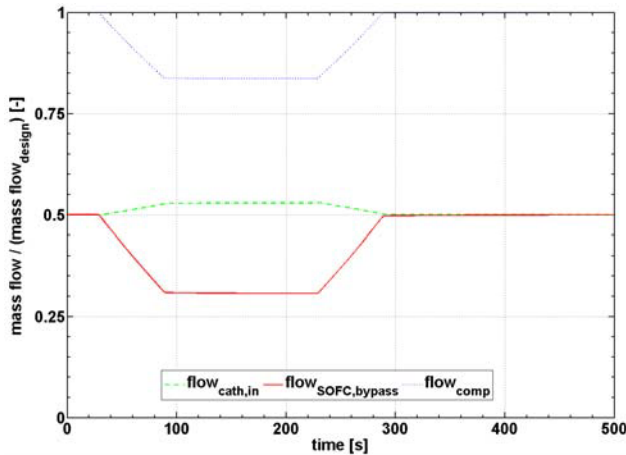


FIG 6. Mass flows through different stations of the hybrid system for a small load change

Safe handling of a hybrid system without using the SOFC bypass would be more complicated compared to the additional control possibility when varying the air flow around the SOFC stack. In this case the MGT controller would ensure safe operation of the stack by varying the air flow through the stack by adjusting the MGT power output [13]. This in fact has a negative impact on the control loop for SOFC power.

6.2. Big load-change / Shutdown

The shutdown manoeuvre of the hybrid system is the biggest possible load-change beginning at the design point condition. Therefore, the simulation results for a big load change are discussed together with a simulated shutdown. The complex manoeuvre is split into several parts: a first change in load down to a power output of approximately 25% followed by the SOFC cut-off and gradual ramp down of the system.

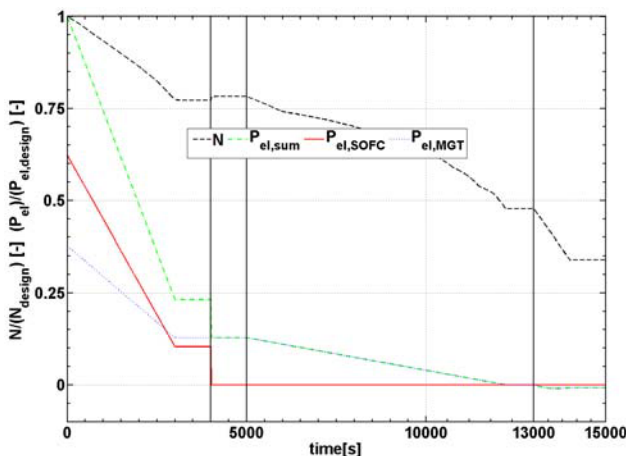


FIG 7. Relative shaft speed and electrical power output for the shutdown procedure

6.2.1. Phase 1: Big load-change

In this first step, the power output of the hybrid system is lowered by 75% within 4000 seconds, which means both SOFC and MGT have to ramp down to part load-points. During this manoeuvre the SOFC cathode outlet temperature needs to be decreased without violating the time gradient. The temperature traces which are shown in FIG 8 demonstrate that this has been achieved.

The cathode outlet temperature follows their specified ramp well (FIG 8). The simulation of the mass flow through/around the cathode side of the SOFC, displayed in FIG 10, results from the output of the temperature control loop for the SOFC and is regulated by adjusting the opening degree of the SOFC bypass valve. The reason for the unexpected time dependant change of the mass flow is the method of calculating the correlation between current density and cell voltage in the SOFC module. To have a reduced calculation time, there are no more discretisations than inlet and outlet of anode and cathode. So the nonlinearities in the used relation between (electrolyte) temperature and resulting ohmic losses [11] have a direct effect on the current-density, respectively the power output. Since both of these values are inputs to the control system, there is no other way to fulfil the law of energy conservation than to adapt the mass flow to the described nonlinearities.

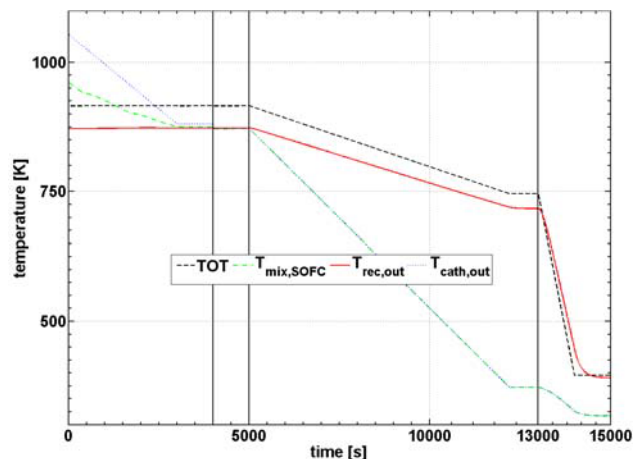


FIG 8. Air-Temperatures around the SOFC-stack and TOT for the shutdown procedure

6.2.2. Phase 2: SOFC cut-off

At 25% nominal hybrid power output, the SOFC is stopped within a stop time of 10 seconds. During this second phase ($t=4000$ secs to $t=5000$ secs), the power output of the gas-turbine is controlled to the constant final load-point of phase one.

Within the first 10 seconds of this phase, several valves are actuated in feed-forward control. The SOFC fuel valve is closed and the purge gas valve is opened simultaneously. At the same time the bypass around the SOFC is closed (FIG 10), which means all available air is flowing through the SOFC cathode. This is necessary for successful cool down of the stack since no more energy is conducted from the stack. The SOFC bypass will not be

used for the rest of the shutdown procedure. The temperature simulation in FIG 8 shows that there is no increase in temperature. Temperatures decrease due to a greater cooling potential.

Furthermore, a small increase of the shaft speed can be determined in FIG 7 and also in FIG 11 as a small kink in the working-line. This phenomenon results from the closure of the SOFC bypass which causes a change in the pressure drop between compressor and turbine resulting in a bigger air flow through the compressor (FIG 10) and hence an increased shaft speed (FIG 7).

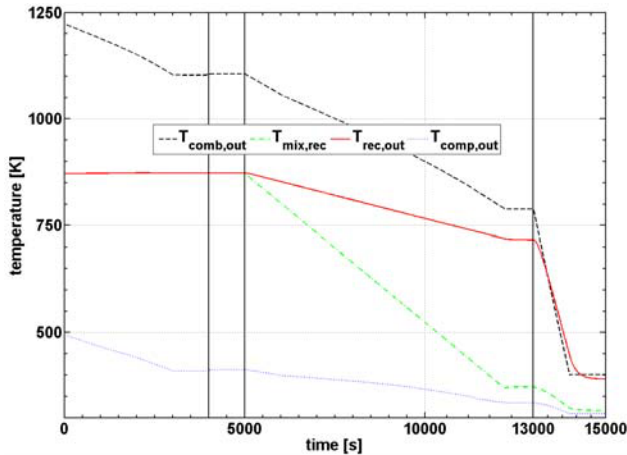


FIG 9. Air-Temperatures around the recuperator and compressor for the shutdown procedure

6.2.3. Phase 3: Bypassing the recuperator

In this phase ($t=5000$ secs to $t=13000$ secs) the bypass around the recuperator of the MGT is used to reduce the stack temperature with feed-back control. This is the only control loop still valid for the SOFC. The remaining loops control the MGT power output and TOT. The bypass mixing temperature after cathode outlet ($T_{mix,SOFC}$) and the cathode outlet temperature ($T_{cath,out}$) are the same (FIG 8) since the SOFC bypass is completely closed.

The objective of this phase is to cool down the inactive but still hot stack. At the end of the phase ($t=13000$ secs), zero power output of the MGT and a shaft speed below 50% should be available. The reason for this is, that for a further cooling down the starter motor of the MGT is necessary and this motor typically cannot run faster than 50% of the design shaft speed.

Since the cathode outlet temperature is lowered at about 500 Kelvin during this phase (FIG 8), the duration should be not shorter than two hours to fulfil the limitation of a maximal time gradient. Similar to the first phase, the power output is lowered in a ramp. The command for the TOT has also to be reduced to achieve a shaft speed below 50%.

The control activity of the recuperator bypass can be read from FIG 10. Here the flow through this bypass starts at 5000 seconds, raises up slowly, and reduces parallel to the compressor flow. At the end of the phase, the flow through the recuperator is only about 10% of the compressor flow.

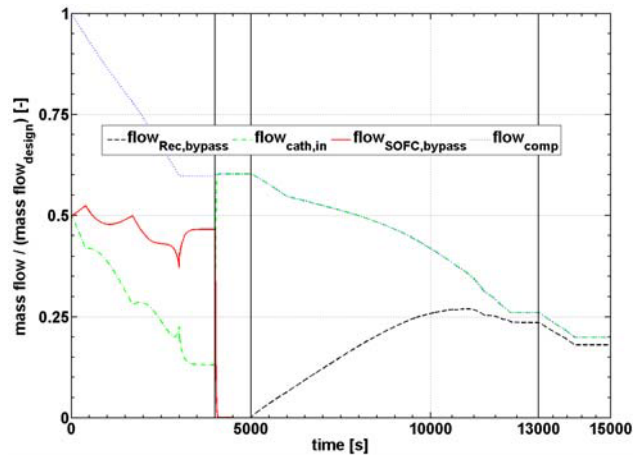


FIG 10. Station mass flows of the hybrid system for the shutdown procedure

6.2.4. Phase 4: Ramp down to ignition shaft speed

In the last phase ($t=13000$ secs to $t=15000$ secs) the first part of the MGT power controller is disabled, and the shaft speed is ramped down to about 35%, which corresponds to the ignition shaft speed of the gas turbine. At same time the TOT is lowered in a ramp by adjusting the fuel flow.

The control loop for the recuperator bypass is no longer in use; the valve stays at the same split than at the end of phase 3.

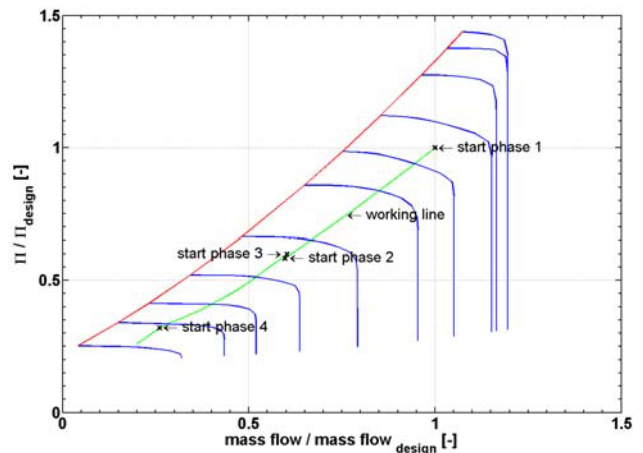


FIG 11. Gas turbine compressor map and working line for the shutdown procedure of the hybrid system

The speed ramp and the power supplied to the shaft by the starter motor are displayed in FIG 7. At the end of Phase 4, the stack temperature is about 320 K (FIG 8). At this time it would be possible to stop the fuel flow to the combustor and control the starter motor to prevent temperatures decreasing too fast.

In the presented simulation, the total time for the shutdown is about four hours. This time could be reduced by shortening the included stabilisation times between the different phases. Since a temperature decrease of about 700 K and more in the SOFC stack had to be achieved

during the shutdown procedure, the time cannot be reduced far below two and a half hours with respect to the maximum time gradient.

CONCLUSIONS

A non-linear Simulink model of a complete SOFC/MGT hybrid system has been developed. A modular model design was chosen to allow simple model improvement and amendment. The hybrid system behaviour has been characterized. The following main conclusions can be drawn:

- With the simple structure of the control system it is possible to run the hybrid model in real-time which is one important objective of the presented work.
- To describe the operation requirements of the hybrid system and especially for the SOFC a list of limitations and boundary conditions need to be fulfilled by any control system.
- Introducing a SOFC bypass enables a better handling of power load changes due to certain decoupling of the SOFC and the MGT. As shown during small load changes, the power change can be covered by the gas turbine only without changing the load conditions at the SOFC. For small load adjustment the SOFC bypass allows that the controlled temperatures of MGT and SOFC remain unchanged.
- A possibility for a shutdown control strategy (4 phases) is proposed which enables successful controlled shutdown without exceeding the given limitations down to a shaft speed of 35%.
- An additional bypass around the recuperator is proposed to cool down the stack temperature after SOFC cut-off.
- During all phases of the system shutdown the important time gradient of the stack temperature (cool-down of the SOFC) is within the limit. Based on the simulation results of time dependant changes all observed parameters behave acceptable.
- For all manoeuvres sufficient simulated compressor surge margin can be demonstrated.

The support and financial sponsorship of this work from the Virtual Institute of Hybrid Power Plant as part of the Helmholtz Association is gratefully acknowledged.

REFERENCES

[1] Achenbach, E., Riensche, E., 1994, "Methane/steam reforming kinetics for solid oxide fuel cells", *Journal of Power Sources* 52 pp.283-288.

[2] Breit, J., Boeing Systems Concept Center, Boeing Commercial Airplanes, "Fuel Cell APU for Commercial Aircraft".

[3] Ferrari, M.L., Traverso, A., Massardo, A.F., 2004, "Transient Analysis of Solid oxide fuel cell hybrids. Part B: Anode recirculation model", ASME paper GT2004-53716, Vienna.

[4] Hörl, F., 1987, "Systemtheoretische Methode zur dynamischen Zustandsüberwachung von Gasturbinen", Doctoral Thesis, TU Munich

[5] Kim, T.S., Yang, W.J., Sohn, J.L., Kim, J.H., Ro, S.T., 2005, "Comparative Performance Assessment of Pressurized Solid Oxide Fuel Cell / Gas Turbine Hybrid System Considering Various Design Options", ASME Paper, GT2005-68533, Reno.

[6] Magistri, L., Bozzolo, M., Tarnowski, O., Agnew, G., Massardo, A.F., 2003, "Design and Off-Design Analysis of a W Hybrid System based on Rolls-Royce Integrated Planar SOFC", ASME paper GT2003-38220, Atlanta.

[7] Magistri, L., Ferrari, M.L., Traverso, A., Costamagna, P., Massardo, A. F., 2004, "Transient Analysis of Solid Oxide Fuel Cell Hybrids Part C. Whole-Cycle Model", ASME Paper GT2004-53845, Vienna.

[8] Magistri, L., Trasino, F., Costamagna, P., 2004, "Transient Analysis of Solid oxide fuel cell hybrids. Part A: Fuel cell models", ASME paper GT2004-53842, Vienna.

[9] Massardo, A.F., 2003 "Analysis of Pressurized Hybrid Systems Based on Rolls-Royce IP-SOFC", ASME Paper GT2003-38220, Atlanta.

[10] Moran, M.J., Shapiro, H.N., 2004, "Fundamentals of Engineering Thermodynamics", 5th ed., Wiley.

[11] Nisancioglu, K., 1989, "Natural gas fuelled solid oxide fuel cells and systems – ohmic losses", International Energy Agency, Workshop on Mathematical Modelling, Charmey, Switzerland.

[12] Srivastava, N., 2006, "Modelling of Solid Oxide Fuel Cell / Gas Turbine Hybrid Systems", Master Thesis, Florida.

[13] Stiller, C., 2006, "Design, Operation and Control Modelling of SOFC / GT Hybrid Systems", Doctoral Thesis, NTNU, Trondheim.

[14] Veyo, S.E., Shockling, L.A., Dederer, J.T., Gillett, J.E., Lundberg, W.L., 2000, "Tubular Solid Oxide Fuel Cell / Gas Turbine Hybrid Cycle Power Systems – Status", ASME Paper, 2000-GT-550, Munich.